Laves phase evolution in a modified P911 heat resistant steel during creep at 923 K

A. Kipelova*, A. Belyakov, R. Kaibyshev

Belgorod State University,

A B S T R A C T

The evolution of $Fe_2(W, Mo)$ Laves phase in a 3%Co modified P911 heat resistant steel was examined during creep tests at 923 K. The tempered martensite lath structure evolved after heat treatment was characterized by dispersion of MX carbonitrides and $M_{23}C_6$ carbides. Appearance of Laves phase particles was recorded after a creep strain of 1%. The mean size of Laves phase particles increased from 190 to 265 nm with increasing strain to 18%. The Laves phase particles were spaced on various boundaries including low-angle boundaries (LABs) of laths/subgrains, but most of these particles (about 90%) were located on high-angle boundaries (HABs) at all strains studied. The size of Laves phase particles located on HABs was larger and their coarsening kinetics was faster than those precipitated on LABs. It is assumed that the evolution of Laves phase during creep is controlled by the grain boundary diffusion of tungsten and molybdenum.

1. Introduction

The 9–12% chromium heat resistant steels have successfully been used for boiler components and turbine rotors of ultra super critical power plants [1–4]. The service properties of martensitic steels are achieved by a complex alloying that provides solution and dispersion strengthening. The solid solution strengthening is provided by the additions of W, Mo, Cr, Co. On the other hand, the elements, such as V, Nb, N and C contribute to the formation of homogeneously distributed fine precipitates, which strengthen and stabilize the tempered microstructure. After tempering, the heat resistant steels usually contain two types of particles: $M_{23}C_6$ carbide and MX carbonitride [5,6]. The $M_{23}C_6$ carbides mainly precipitate along high and low-angle boundaries and they act as obstacles for migrating boundaries. Efficiency of $M_{23}C_6$ particles in stabilizing tempered martensite lath structure (TMLS) degrades with service duration, since they tend to coarsen during creep at elevated temperatures. It was recently shown [1,7,8] that this is a key factor restricting creep resistance of martensitic steels. Homogeneously distributed fine MX carbonitrides are more stable at operating temperatures as compared to $M_{23}C_6$ particles. After rather long ageing and/or creep, relatively large particles of Laves phase appear in martensitic steels [9–14]. Laves phase being thermodynamically equilibrium one precipitates at temperatures below about 973 K during creep exposure or isothermal ageing and results in removing the W and Mo from the solid solution [9,14,15]. A lot of work has been conducted to study the effect of Laves phase on stability of microstructures and strength of steels during creep [9–15]. It is assumed that the fine precipitates of Fe_2W Laves phase effectively decrease the creep rate in the transient region [14]. In other words, the fine Laves phase particles may contribute to dispersion hardening [3,14,15]. The significant contribution to dispersion strengthening from Laves phase particles can be expected in the case of their homogeneous precipitation throughout ferritic matrix. However, there is no experimental evidence for homogeneous precipitation of Laves phase. It was also pointed out that extensive coarsening of Laves phase promotes the acceleration or increase of creep rate after reaching a minimum creep rate [14]. The dispersion strengthening owing to precipitations of Laves phase compensates for the depletion of W from solid solution in the transient creep, but coarse particles of Laves phase along with W-deficient solid solution accelerate the creep rate at sufficiently large strains [9].

In spite of numerous papers, the precipitation sites for Laves phases have not been studied in sufficient detail, although this is a key issue to establish the role of Laves phase on creep resistance of martensitic steels. Sawada et al. suggested that Laves phase (Fe_2Mo) particles in Mod.9Cr–1Mo steel precipitate on high-angle boundaries (HAB) of prior austenite grains (PAG) and packet boundaries in martensitic lath structure, while Fe_2W particles in TAF650 steel precipitate on lath boundaries, thereby retarding

the recovery of lath structure and increasing the creep rupture strength [16]. Particles of Laves phase located on HABs scarcely contribute to the dispersion hardening. However, Laves phase precipitations on low-angle boundaries (LABs) of martensite laths should improve their efficiency to act as barriers for dislocation motion, leading to additional structural strengthening. The aim of the present work is to clarify the precipitation sites for $Fe_2(W, Mo)$ Laves phase and investigate their evolution in a 3%Co modified P911 heat resistant steel during creep at 923 K.

2. Experimental procedure

A 3%Co modified P911-type steel (0.13%C, 8.6%Cr, 3.2%Co, 1.15%W, 0.93%Mo, 0.2%V, 0.1%Cu, 0.07%Nb, 0.06%Si, 0.05%Ni, 0.04%N, 0.02%Mn, 0.005%B, all in mass%, and the balance Fe) was examined. The steel ingot was hot forged at 1373 K to a square bar of 25 mm × 25 mm. Then, the steel forging was austenitized at 1323 K for 0.5 h followed by air cooling and tempered at 1023 K for 3 h. Flat specimens having a cross section of 7 mm × 3 mm and 25 mm gauge length were used for creep tests. The creep tests were carried out at 923 K with initial stress of 118 MPa, to strains of 1% (374 h), 4% (1654 h), 6% (2960 h) and to rupture (4743 h) in order to study the evolution of Laves phases at various creep stages.

The microstructural investigations were carried out on longitudinal section of crept specimens within the gauge length by using a Quanta 600 FEG scanning electron microscope (SEM) incorporating an orientation imaging microscopy (OIM) system and an X-ray energy-dispersive spectrometer (EDS). The SEM specimens were prepared by electro-polishing method with a 10% solution of perchloric acid in glacial acetic acid. The OIM maps of dimension of 50 μm × 50 μm were obtained under the following conditions: accelerating voltage of 20 kV, beam current of 18 nA, working distance of 10 mm, step size of 50 nm. The grain boundaries with misorientations of $\theta \geq 15^\circ$ and $2^\circ < \theta < 15^\circ$ were considered as HABs and LABs, respectively. The HABs are depicted in the OIM images as black lines, and the LABs are indicated by white lines. An area of 30 μm × 26 μm was scanned with BSE (back scattered electron) detector for each sample. The Laves phase could be clearly distinguished from other precipitates by its bright contrast in the BSE image (Z-contrast) [17]. The particles of Laves phase were identified by using *Z*-contrast technique as well as by chemical composition. The amounts of Fe, Cr, W, and Mo, were measured for the chemical analysis. A particle was considered as Laves phase if the total content of tungsten and molybdenum comprised 30–35 at%. A total of 150–300 particles of Laves phase was analyzed for each data point.

3. Results and discussion

3.1. Creep behavior

Fig. 1 shows the creep rate versus creep strain curve of the P911 + 3%Co steel at 923 K and under nominal stress of 118 MPa. The curve consists of the transient creep region extending up to a strain of 1%, and after reaching a minimum creep rate at strain of about 2% the region of accelerated creep takes place at strains beyond 6%. The creep behavior is characterized by an almost constant creep rate of about $2 \times 10^{-5}\ h^{-1}$ in the strain range of 1–6%, suggesting that an apparent steady-state flow takes place. In order to clarify the evolution of Laves phase during creep the microstructures were studied in the samples crept to some characteristic strains indicated by arrows in Fig. 1.

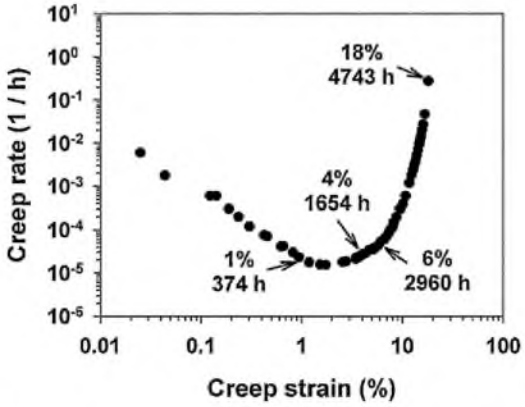

Fig. 1. Creep rate *vs.* creep strain curve for the P911 + 3%Co steel at 923 K.

3.2. Microstructures after creep tests

Typical microstructures that evolved in the gauge portions of samples subjected to creep at 923 K to different strains are shown in Fig. 2 as a series of OIM and SEM–BSE images. The SEM–BSE images correspond to the indicated portions in OIM micrographs. The microstructures of P911 + 3%Co steel consist of the PAGs, which are subdivided by HABs of packets and blocks and LABs of laths (Fig. 2). The Laves phase particles are observed after relatively small strain of 1% (the creep duration is 374 h). Therefore, the crept microstructures are characterized by a dispersion of MX carbonitrides, $M_{23}C_6$ carbides and relatively large Laves phase particles. The Laves phase particles can be uniquely distinguished from any other precipitates by their bright contrast in the SEM–BSE images (Fig. 2 b, d, f and h). Fig. 3 shows the corresponding EDS analysis for these particles, confirming that the chemical composition is consistent with Laves phase. It is seen that precipitation of Laves phase occurs in highly heterogeneous manner; interiors of martensite laths are almost free of Laves phase particles. Almost all Laves phase particles locate on various boundaries. The most of the particles (about 90%) precipitated on HABs at the all strain levels (Table 1). Precipitation of Laves phases on grain/subgrain boundaries have been observed in other studies on martensitic creep resistant steels [3,6,14]. The prevalent precipitation at HABs may be associated with somewhat increased diffusivity of constitutive elements along ordinary grain boundaries. However, this interesting topic should be further clarified.

Table 1
Laves phase particles in 3%Co modified P911 steel after creep tests at 923 K.

Creep strain	1% (374 h)	4% (1654 h)	6% (2960 h)	Ruptured (4743 h)
Size of particles (nm)	185	188	245	265
Aspect ratio of particles	1.9	1.8	1.8	1.8
Size of particles located on LABs (nm)	155	187	176	225
Aspect ratio of particles located on LABs	2.0	1.9	1.7	1.5
Size of particles located on HABs (nm)	188	188	253	272
Aspect ratio of particles located on HABs	1.9	1.8	1.8	1.8
Volume fraction of particles (%)	0.85	1.42	2.2	2.0
Volume fraction of particles located on LABs (%)	7	12	7.7	7.8
HABs (%)	62.5	60	53.7	57.6

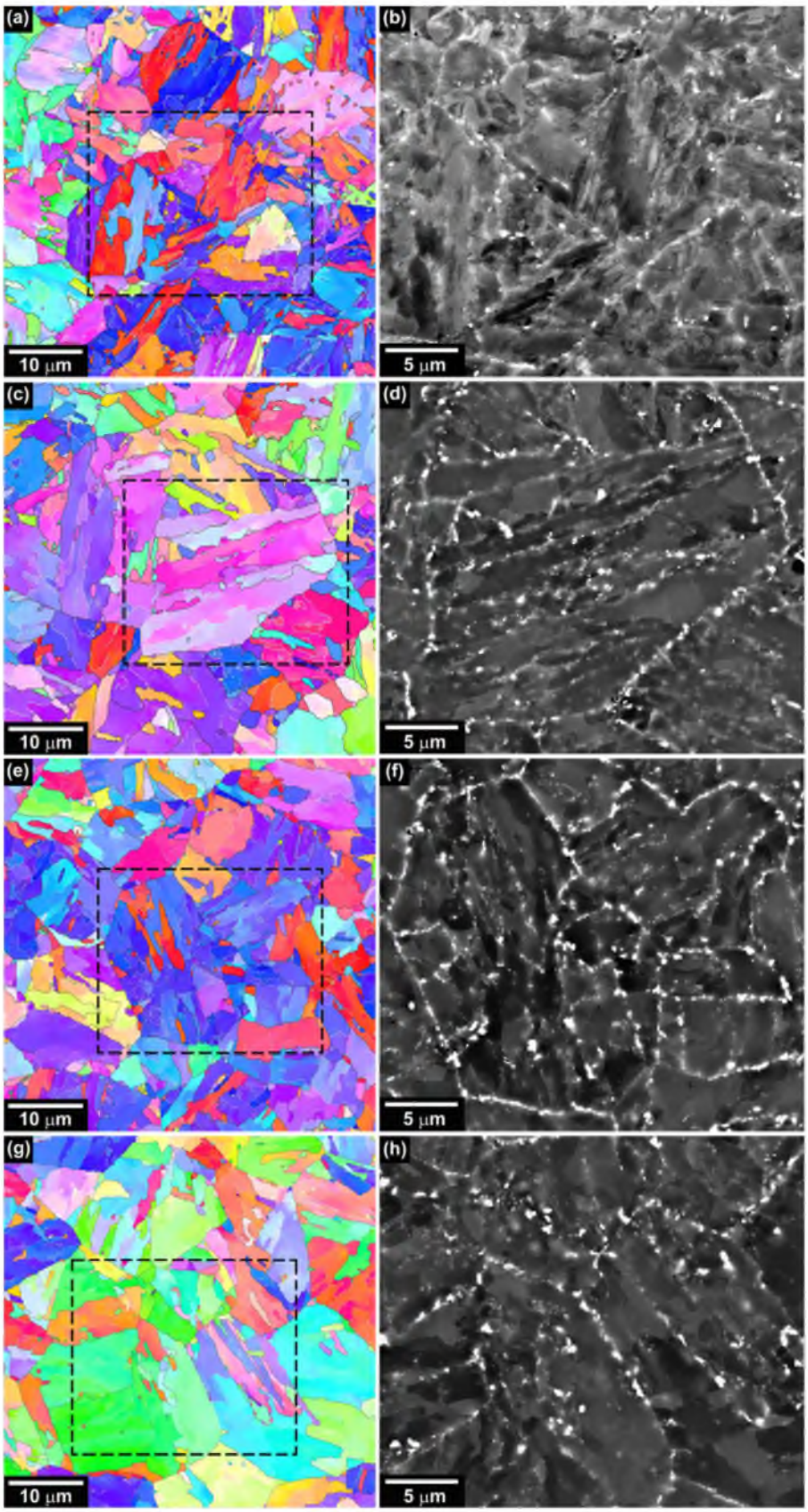

Fig. 2. Microstructure of the 3%Co modified P911 steel in gauge portions after creep tests at 923 K; OIM micrographs (a, c, e and g) and SEM–BSE images (b, d, f and h) showing location of Laves phase at creep strains of 1% (a and b), 4% (c and d), 6% (e and f) and in ruptured specimen (g and h).

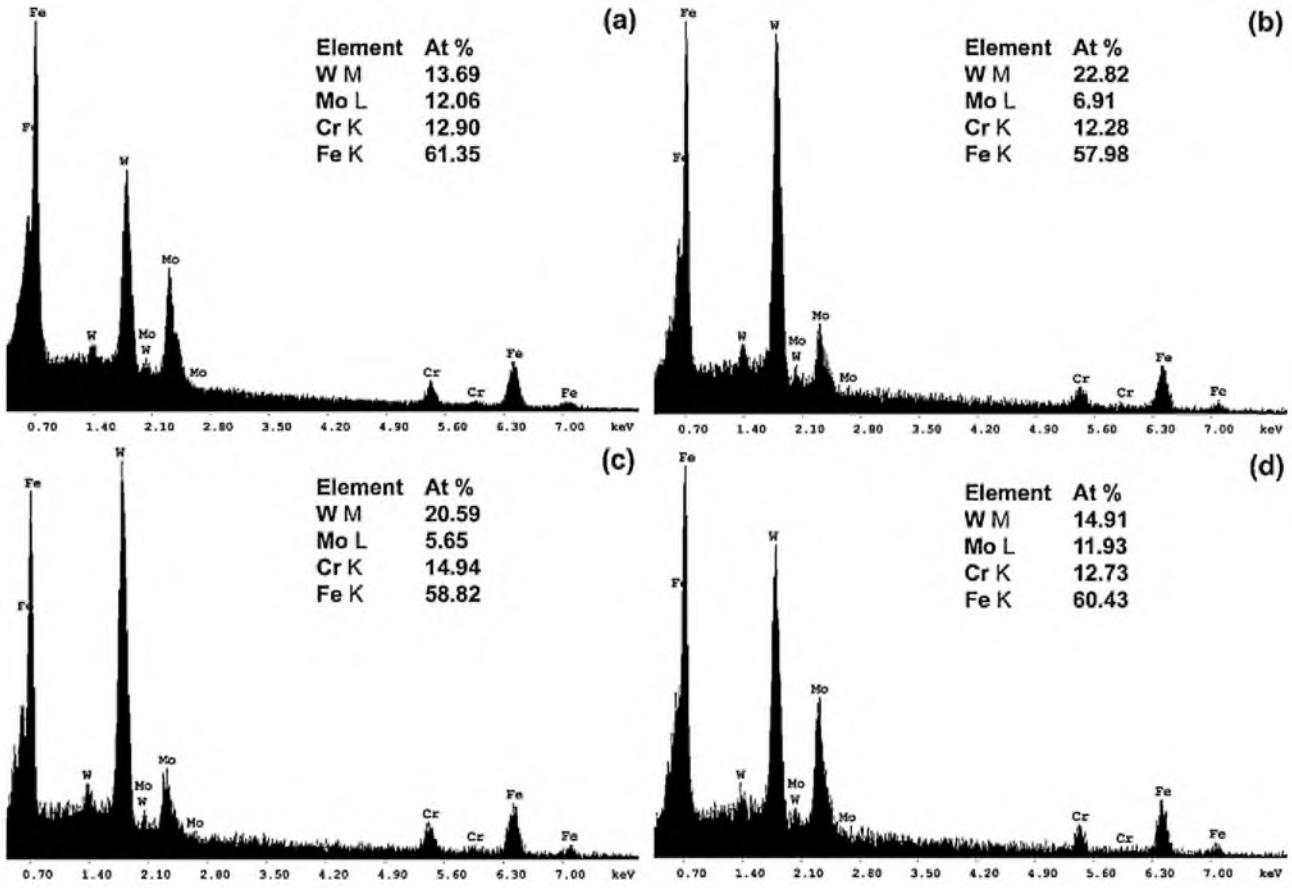

Fig. 3. EDS analysis showing the chemical composition of Laves phases at creep strains of 1% (a), 4% (b), 6% (c) and in fractured specimen (d).

The volume fraction of Laves phase increases from 0.85% to 2.2% with increasing the strain from 1% to 6% (Table 1). Further straining up to rupture is not accompanied by the change of the volume fraction of Laves phase that remains almost constant at a level of about 2%. This is consistent with another study on the Laves phase precipitation kinetics [9], which suggested that the equilibrium fraction is reached after about 2000 h. It should be noted that the fraction of HABs does not change remarkably with straining (Fig. 2 a, c, e, g and Table 1). Despite the fact that portion of LABs is about 40% at all strains the volume fraction of Laves phases located on these boundaries does not exceed 12%. Therefore, most of Laves phase precipitates concurrently on HABs of PAGs, packets and blocks under creep exposure.

Examination of the chemical composition of Laves phase particles shows that these particles are enriched with tungsten (Fig. 3). However, the Mo/W ratio varies in the particles during creep (Fig. 4). The quantities of tungsten and molybdenum in the Laves phases are almost the same at early creep to a strain of 1%. Then, the ratio of Mo/W drops to about 0.3 at creep strains of 4 and 6%. Finally, the Mo/W ration comprises 0.77 in the specimen crept to failure. Relatively high amount of molybdenum in the Laves phase at low strains may result from high diffusivity of molybdenum as compared to tungsten [18,19]. All available Mo atoms spaced vicinity of grain/subgrain boundaries rapidly precipitate as Laves phases enriched with Mo. Increase in the tungsten content at moderate strains is, probably, associated with lower enthalpy for the formation of Fe_2W instead of Fe_2Mo. After rather long exposure for 4743 h at 923 K, the ratio of Mo/W in the Laves phase approaches a value of 0.8 that is probably affected by a rather large molybdenum/tungsten value of 1.4 in the studied steel.

3.3. *Distribution and growth kinetics of Laves phases*

Fig. 5 shows the changes in the size distributions of Laves phases located on different boundaries with increasing the creep strain. After strains of 1% and 4% (Fig. 5a and d), the charts plotted for the particles located at HABs show diffuse peaks at particle size of 50–400 nm with maximum against about 100 nm. The peaks spread out toward the larger sizes up to 700 nm and their heights decrease with increasing the creep strain (Fig. 5g and j). The flat-like size distribution of Laves phase particles with almost the same quantities of particles of various sizes evolves in the specimen crept to failure. In contrast to the size distributions of Laves phases located at HABs, the particles of Laves phase located on LABs are characterized by sharper peaks, especially at strains below 6%. The most of particles have size ranging from 100 to 300 nm (Fig. 5b, e, h and k). The changes in the size distributions during the creep are associated with a gradual motion of the peak size from about 100 nm to 200 nm with increase of the strain from 1% to rupture. Since the majority of Laves phase particles is situated on HABs, the total size distribution of the particles precipitated at all boundaries irrespective of misorientations is similar to that one obtained for HAB precipitates. The diffuse peak at particle size of 100–400 nm that evolved at early creep stage expands to larger sizes with the test duration (Fig. 5c, f, i and l). It is worth noting that the particles are somewhat elongated along the boundaries; the aspect ratio is about 1.8 for all studied strain levels (Table 1).

Fig. 6 shows the quantitative analysis of the effect of creep time on the growth of Laves phases located on LABs and HABs. Commonly, the particle growth behavior is expressed by a power law function of exposure time: $d = Kt^{1/n}$, where d is the average grain diameter, t is the isothermal annealing time, n is a growth

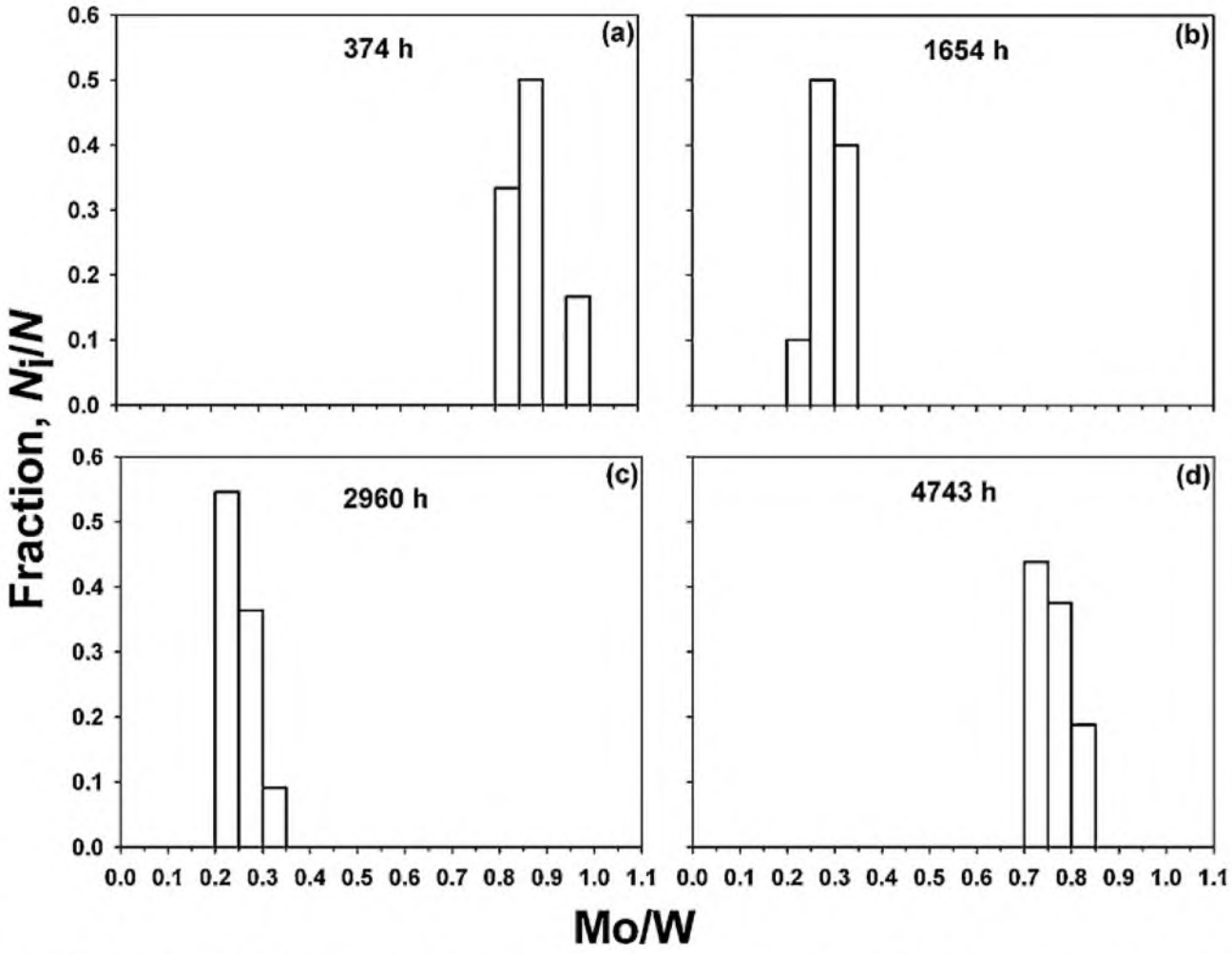

Fig. 4. The measured ratio of molybdenum to tungsten in the Laves phase particles at various creep strains of 1% (a), 4% (b), 6% (c) and in fractured specimen (d).

exponent and K is constant [20]. The size of Laves phases can be related to the creep time through power-law expressions with the particle growth exponents (n) of about 6.7 and 8.3 for particles located on HABs and LABs, respectively (Fig. 6). The size of Laves phase particles located on HABs is remarkably larger than those spaced on LABs. Moreover, the Laves phases located on HABs are characterized by a faster kinetics of their growth. The size of Laves phase particles comprised 170 nm after creep at 600 °C for almost the same time [21]. Therefore, the activation energy for the particle growth is calculated as 60 kJ/mole, which is less than half of the activation energy for volume diffusion of tungsten (216 kJ/mole [18]). This suggests that the evolution of Laves phase during creep is assisted by a grain boundary diffusion processes. The elongated shape of the particles also implies an important role of boundary diffusion in both the precipitation and the growth.

Increase in the mean size of Laves phase particles by a factor of 1.3, i.e. from 185 to 245 nm, in the range of creep strains of 1–6% is accompanied by more than twofold increase of their volume fraction. It can be concluded, therefore, that the growth of Laves phase particles during creep to a strain of 6% takes place by continuous precipitation. The growth of precipitated particles takes place concurrently with the appearance of newly developing precipitates. On the other hand, the volume fraction of Laves phase scarcely changes in the range of relatively large strains above 6%, when the test duration time exceeds 3000 h. The particle growth under conditions of invariant volume fraction suggests that the coarsening occurs by a mechanism of coagulation; namely, relatively large particles grow at expense of finer ones. Particles of Laves phase located on HABs have a priority in the coarsening due to fast grain boundary diffusion. Takahashi et al. [22] pointed out that Laves phase with tungsten as the major component grew rapidly than Laves phase with molybdenum. In the present study, however, any remarkable effect of the Mo/W ratio on the coarsening behavior of Laves phase particles was not revealed.

The appearance of Laves phases on grain/subgrain boundaries as revealed in the present study unambiguously testifies to their heterogeneous nucleation during long-term creep at elevated temperatures. The precipitation of Laves phase on various boundaries enhances the stability of the tempered martensite structure against coarsening that should improve the creep resistance of steel that is extremely important for creep resistance of martensitic steel. However, Laves phase hardly contribute to dispersion strengthening. In addition, relatively small amount of Laves phase particles precipitated on LABs could not increase significantly the structural strengthening originated from lath boundaries. The formation of Laves phases removes the tungsten and molybdenum from solid solution, resulting in deterioration of the solid solution strengthening of ferrite matrix [9,14,15]. Moreover, the most of Laves phase particles precipitate on HABs, whereas the creep resistance of martensitic steels depends on the stability of lath substructure. Therefore, the effect of Laves phases on the creep properties of martensitic steels is negative rather than positive.

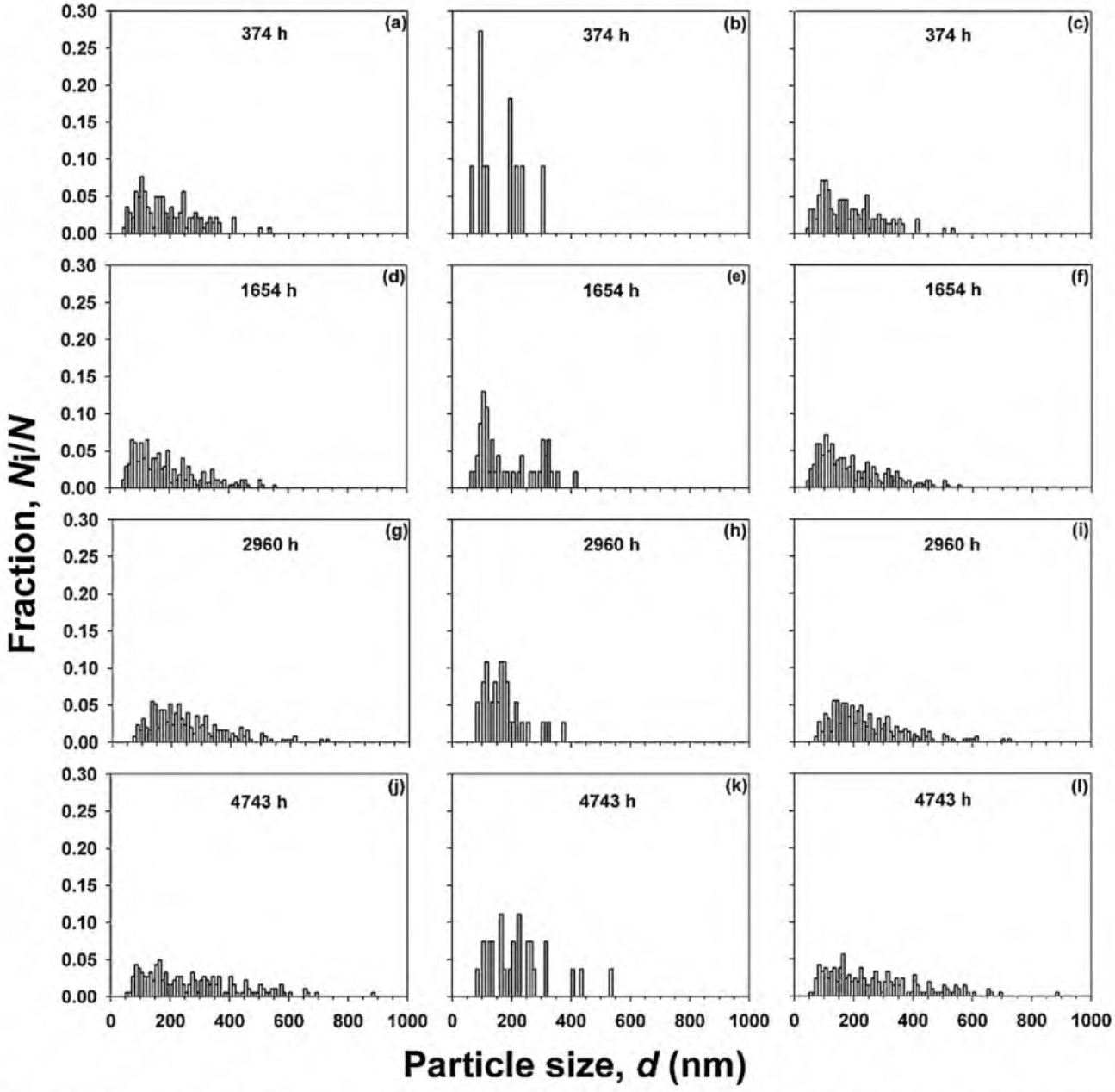

Fig. 5. Particle size distributions for Laves phases at creep strains of 1% (a–c), 4% (d–f), 6% (g–i) and in fractured specimen (j–l); (a, d, g and j) Laves phases located on HABs; (b, e, h and k) Laves phases located on LABs; (c, f, i and l) total size distribution of Laves phases.

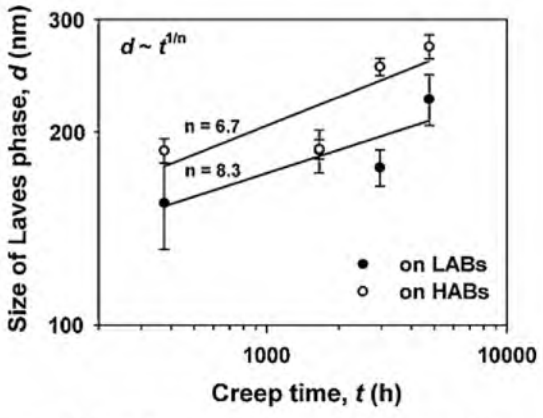

Fig. 6. Effect of creep time on the mean size of Laves phases.

4. Conclusions

Evolution of $Fe_2(W,Mo)$ Laves phase in a 3%Co modified P911 heat resistant steel was examined during creep tests at 923 K. The main results can be summarized as follows.

(1) Most of the Laves phase particles appear on high-angle boundaries of prior austenite grains and martensite blocks/packets, while about 10% of the particles only precipitate on low-angle boundaries of martensite laths/subgrains irrespective of creep stages.
(2) The volume fraction of Laves phase increases from 0.85% to 2.2% with increasing the strain from 1% to 6%; and after strain of 6% (2960 h) the volume fraction of Laves phase remains constant during further creep up to rupture.
(3) The Laves phase particles are characterized by a diffuse size distribution, which extends from about 50 to 400 nm at early

precipitation stage and spreads to 700 nm in the specimen crept for 4743 h.

(4) The Laves phase precipitates on high-angle boundaries are larger and demonstrate faster kinetics of growth than those precipitated on low-angle subboundaries. The sizes of Laves phase particles can be expressed by power law functions of creep time with grow exponents of 6.7 and 8.3 for the particles located on high and low-angle boundaries, respectively.

Acknowledgements

This study was supported by Ministry of Education and Science, Russia, under grant no. 02.740.11.0119. Authors are grateful to staff of Joint Research Centre, Belgorod State University, for their assistance with structural and mechanical characterizations.

References

[1] R.O. Kaybyshev, V.N. Skorobogatykh, I.A. Shchenkova, Phys. Met. Metall. 109 (2010) 186–200.
[2] B. Sonderegger, S. Mitsche, H. Cerjak, Mater. Sci. Eng. A481–482 (2008) 466–470.
[3] J. Hald, L. Korcakova, ISIJ Int. 43 (2003) 420–427.
[4] M. Hattestrand, M. Schwind, H.-O. Andren, Mater. Sci. Eng. A250 (1998) 27–36.
[5] M. Taneike, K. Sawada, F. Abe, Metall. Mater. Trans. 35 (2004) 1255–1261.
[6] K. Maruyama, K. Sawada, J. Koike, ISIJ Int. 41 (2001) 641–653.
[7] A. Kipelova, R. Kaibyshev, A. Belyakov, D. Molodov, Mater. Sci. Eng. A 528 (2011) 1280–1286.
[8] J. Hald, Int. J. Pressure Vessels Piping 85 (2008) 30–37.
[9] O. Prat, J. Garcia, D. Rojas, C. Carrasco, G. Inden, Acta Mater. 58 (2010) 6142–6153.
[10] H. Cui, F. Sun, K. Chen, L. Zhang, R. Wan, A. Shan, J. Wu, Mater. Sci. Eng. A 527 (2010) 7505–7509.
[11] A. Aghajani, F. Richter, C. Somsen, S.G. Fries, I. Steinbach, G. Eggeler, Scr. Mater. 61 (2009) 1068–1071.
[12] A. Aghajani, Ch. Somsen, G. Eggeler, Acta Mater. 57 (2009) 5093–5106.
[13] Q. Li, Metall. Mater. Trans. 37 (2006) 89–97.
[14] F. Abe, Metall. Mater. Trans. 36 (2005) 321–332.
[15] G. Qin, S.V. Hainsworth, A. Strang, P.F. Morris, P.D. Clarke, A.P. Backhouse, TEM studies of microstructural evolution in creep exposed E911//creep & fracture in high temperature components, in: 2nd ECCC Creep Conference, DEStech Publications, 2009, pp. 889–899.
[16] K. Sawada, M. Takeda, K. Maruyama, R. Ishii, M. Yamada, Y. Nagae, R. Komine, Mater. Sci. Eng. A267 (1999) 19–25.
[17] G. Dimmler, P. Weinert, E. Kozeschnik, H. Cerjak, Mater. Charact. 51 (2003) 341–352.
[18] R.A. Perez, D.N. Torres, Appl. Phys. A (2010), doi:10.1007/s00339-010-6142-x.
[19] A.D. LeClaire, G. Neumann, in: H. Mehrer (Ed.), Diffusion in Solid Metals and Alloys, Springer-Verlag, 1990, pp. 124–130.
[20] P.A. Beck, J. Appl. Phys. 18 (1947) 1028–1029.
[21] A.Yu. Kipelova, A.N. Belyakov, V.N. Skorobogatykh, I.A. Shchenkova, R.O. Kaibyshev, Met. Sci. Heat Treat. 52 (2010) 118–127.
[22] T. Takahashi, T. Wakai, N. Aoto, Curr. Adv. Mater. Process. 18 (2005) 1618.